

**FUNDAMENTAL STUDIES ON THE
MECHANISM OF *Polyalthia longifolia* (Sonn.)
Thwaites POLYPHENOLS ACTION IN HELA
CELLS IN RELATION TO MICRORNA
REGULATION**

by

VIJAYARATHNA SOUNDARARAJAN

**Thesis submitted in fulfilment of the requirements
for the degree of
Doctor of Philosophy**

May 2017

ACKNOWLEDGEMENT

It would not have been possible to complete this PhD thesis without the help and support of the kind people around me, to only some of whom it is possible to give particular mention here. Above all, I would like to thank my parents, brothers and sisters for their personal support and great patience at all times. As for my husband, Sugesh, words go insufficient in expressing my gratitude ever since he became my pillar of strength throughout course.

This thesis would not have been possible without the help, support and patience of my main supervisor, Associate Professor Dr. Sasidharan Sreenivasan, not to mention his advice and unsurpassed knowledge on medicinal plants. I could not even imagine a better advisor for my research to which his knowledge, understanding, patience, guidance and encouragement has brought me to complete my thesis on time. The good advice, support and friendship of my co-supervisors, Professor Dr. Darah Ibrahim from School of Biological Science and Dr. Oon Chern Ein from Institute for Research in Molecular Medicine (INFORMM), who had served invaluable on both academic and personal perspective, for which I am extremely grateful.

I would also like to acknowledge the Fundamental Research Grant Scheme (FRGS; Grant No.: 203/CIPPM/6711379) from the Ministry of Education Malaysia, Government of Malaysia that provided the necessary financial support for this research. Not to forget the support I received from the Ministry of Education Malaysia, Government of Malaysia, by awarding me with MyPhD fellowship. The research facilities of the Universiti Sains Malaysia as well as the necessary laboratory equipment offered by INFORMM have been indispensable. I also would

like to thank INFORMM again for their support and assistance since the beginning of my postgraduate work, particularly the director of INFORMM, Prof. Norazmi Mohd. Nor.

I am also most grateful to Pn. Jamilah, En. Johari and En. Rizal, from the Electron Microscopy Unit, School of Biological Science, USM for providing me with their expertise in preparations and viewing of SEM and TEM samples. I would also like to thank Pn. Norfadhillah Ya'akob from Advanced Medical and Dental Institute, USM for her help in operating flow cytometry especially concerning the results interpretations and Pn. Uswatun Bahirah from Centre for Chemical Biology (CCB) for her help in RNA quality assessment. Not to mention the help of Mr. Shie Jie Pang and Mr. Zhi Hui from Genomax Technologies Pte Ltd, Singapore who had been providing me with their unlimited guidance over the interpretation of data relating to microRNA sequencing.

Last but not least, I would like to thank my friends from INFORMM, especially Kalaivani, Kavitha, Priya and Sanggetha for their support, guidance and encouragement.

For any error or inadequacies that may remain in this work, of course, the responsibility is entirely my own.

VIJAYARATHNA A/P SOUNDARARAJAN

Institute for Research in Molecular Medicine

Universiti Sains Malaysia

October 2016

TABLE OF CONTENTS

ACKNOWLEDGEMENT	ii
TABLE OF CONTENTS	iv
LIST OF TABLES	xiii
LIST OF FIGURES	xiv
LIST OF PLATES	xviii
LIST OF SYMBOLS AND ABBREVIATIONS	xxi
ABSTRAK	xxiv
ABSTRACT	xxvi
CHAPTER 1.0: INTRODUCTION	1
1.1 Overview and Rationale of Study	1
1.2 Objectives	4
CHAPTER 2.0: LITERATURE REVIEW	5
2.1 Apoptosis	5
2.1.1 Morphological Changes in Apoptosis	5
2.1.2 Biochemical Changes in Apoptosis	6
2.2 Apoptosis Detection Method	7
2.2.1 Detection of Apoptosis through Morphological Analysis	7
2.2.2 Detection of Apoptosis via Flow Cytometry Analysis	9
2.2.3 The Usage of Flow Cytometry in Cell Quantification	10
2.2.4 Detection of Apoptosis via Mitochondrial Membrane Potential (MMP)	11
2.3 Necrosis	12

2.4	Cell Cycle	14
2.4.1	Cell Cycle and Apoptosis	14
2.5	Reactive Oxygen Species (ROS)	16
2.5.1	Reactive Oxygen Species (ROS) and Cancer	17
2.6	MicroRNA	19
2.6.1	Canonical Pathway of miRNA Biogenesis	20
2.6.2	Canonical Pathway of miRNA Biogenesis	23
2.7	Cancer, a Life Threatening Disease	24
2.7.1	Anticancer Substances from Natural Products	26
2.7.2	Modulation of microRNA by Phytochemicals	27
2.8	Plant as Potential Natural Source of Anticancer Agent	31
2.8.1	Selection of Plants	32
2.9	Plant Extracts	33
2.9.1	Extraction of Plants	33
2.10	Botanical Aspects of the Family Annonacea	34
2.10.1	Taxonomical Classification of <i>Polyalthia longifolia</i> (Sonn.) Thwaites	36
2.10.2	Botanical Description of <i>Polyalthia longifolia</i>	37
2.11	Pharmacological Activities and Traditional Usage of <i>P. longifolia</i>	39
2.11.1	The Anti-cancer Property of <i>P. longifolia</i>	40
CHAPTER 3.0: EVALUATION OF CELL CYTOTOXICITY THROUGH <i>IN VITRO</i> ULTRAMORPHOLOGICAL CHANGES AS INDUCED BY <i>Polyalthia longifolia</i> (Sonn.) Thwaites LEAF METHANOLIC EXTRACT (PLME)		42
3.1	INTRODUCTION	42
3.1.1	Objectives	43

3.2	MATERIALS AND METHODS	44
3.2.1	Plant Sample Collection	44
3.2.2	Preparation of PLME	44
3.2.3	Gas Chromatography-Mass Spectrometry (GC-MS) Profiling	45
3.2.4	Cell Line and Culture	45
	3.2.4(a) Culturing Medium for Cell Lines	46
3.2.5	PLME Cytotoxicity Activity	46
	3.2.5(a) Cell Inhibition Assay by 3-(4,5-dimethylthiazol-2-yl)-2,5diphenyl tetrazolium bromide (MTT) Assay	46
	3.2.5(b) Cell Proliferation Assay by CyQUANT	48
3.2.6	Morphological Study of HeLa using Various Methods of Microscopy	48
	3.2.6(a) Light Microscope (LM) Analysis Using Giemsa Stained Cells	48
	3.2.6(b) Morphological Observation through Holographic Digital Microscopy (HDM)	49
	3.2.6(c) Morphological Observation through Scanning Electron Microscope (SEM)	49
	3.2.6(d) Morphological Observation through Transmission Electron Microscope (TEM)	50
3.2.7	Statistical Analysis	50
3.3	RESULTS	51
3.3.1	Extraction of <i>P. longifolia</i> Leaf Yield and Gas Chromatography Mass Spectrometry (GC-MS) Profiling	51
3.3.2	Cytotoxicity Effects of PLME Measured with MTT and CyQUANT	54
3.3.3	Morphological Changes Evaluated by Light Microscopy (LM)	58

3.3.4	Morphological Changes Evaluated by Holographic Digital Microscopy (HDM)	64
3.3.5	Morphological Changes Evaluated by Scanning Electron Microscope (SEM)	71
3.3.6	Morphological Changes Evaluated by Transmission Electron Microscope (TEM)	78
3.4	DISCUSSIONS	85
3.4.1	Preparation of PLME	85
3.4.2	Extraction Yield and Gas Chromatography Mass Spectrometry (GC-MS) Analysis of PLME	89
3.4.3	<i>In vitro</i> Cytotoxicity Assays by MTT and CyQUANT	91
3.4.4	Changes on Cell Morphology Observed in Light Microscope (LM)	96
3.4.5	Cell Morphological Assessment by Holographic Digital Microscopy (HDM)	97
3.4.6	Changes of Morphology as Viewed in Scanning Electron Microscope (SEM)	98
3.4.7	Changes of Morphology as Viewed Through Transmission Electron Microscope (TEM)	101
3.5	CONCLUSIONS	104
CHAPTER 4.0: <i>Polyalthia longifolia</i> (Sonn.) Thwaites METHANOLIC LEAF EXTRACT (PLME) INDUCE P53 MEDIATED APOPTOSIS, CELL CYCLE ARREST AND MITOCHONDRIAL POTENTIAL DEPOLARIZATION BY MODULATING THE REDOX STATUS IN HELA CELLS		105
4.1.	INTRODUCTION	105
4.1.1	Objectives	106
4.2	MATERIALS AND METHODS	107
4.2.1	Plant Extraction and HeLa Cell Culture	107
4.2.2	Flow Cytometry Analysis of Apoptosis/Necrosis by Using Annexin V-FITC/Propidium Iodide (PI) Staining Method	107

4.2.3	Cell Cycle Analysis by Flow Cytometry	108
4.2.4	DCF Assay for Reactive Oxygen Species (ROS) Determination	108
4.2.5	Comet Assay for Potential DNA Damage	110
4.2.6	Measurement of Mitochondrial Membrane Potential ($\Delta\Psi_m$) by using JC-1 Mito Screen Assay	110
4.2.7	Human Apoptotic Proteins Array	111
4.2.8	Flow Cytometry Analysis Affixed under General Condition	112
4.2.9	Statistical Analysis	112
4.3	RESULTS	113
4.3.1	PLME-Induced HeLa Cell Apoptosis using Annexin V/PI Staining and Flow Cytometry Analysis	113
4.3.2	The Effect of PLME Treatment on HeLa Cell Cycle Distribution	117
4.3.3	PLME Induces Mitochondrial Membrane Potential ($\Delta\Psi_m$) in HeLa Cells	122
4.3.4	PLME Induces Intracellular ROS Generation in HeLa Cells	126
4.3.5	PLME Induces DNA Fragmentation in HeLa Cells	129
4.3.6	Effects of PLME on Apoptosis-Related Proteins Expression in HeLa Cells	138
4.4	DISCUSSION	143
4.4.1	Role of Apoptosis in Cancer Therapy	143
4.4.2	Biochemical Assays for Detection of Apoptosis	145
4.4.3	Targeting Phosphatidylserine (PS) Exposure during Apoptosis	146
	4.4.3(a) Flow Cytometry Analysis of Apoptosis in HeLa Cells	147
4.4.4	Cell Cycle and Apoptosis	150
	4.4.4(a) Flow Cytometry Analysis of PLME Effect on Cell Cycle Distribution	151

4.4.5	The Role of Mitochondrial Membrane Potential ($\Delta\Psi_m$) in Apoptosis	153
4.4.5(a)	Flow Cytometry Analysis of PLME Effect on Mitochondria Membrane Potential ($\Delta\Psi_m$)	156
4.4.6	Role of Reactive Oxygen Species (ROS) in Cancer	158
4.4.6(a)	Measurement of Reactive Oxygen Species (ROS) using DCFH-DA	158
4.4.6(b)	PLME Effect on ROS Generation	159
4.4.7	Comet Assay	160
4.4.7(a)	Interpretation of DNA fragmentation as Induced by PLME in HeLa Cells	162
4.4.8	Expression of Apoptotic Proteins through Microarray Analysis	164
4.4.8(a)	Analysis of the Apoptotic Proteins Detection from Raybio Array	166
4.5	CONCLUSIONS	170
CHAPTER 5.0: IDENTIFICATION OF MICRORNAS AND META-ANALYSIS BASED DETERMINATION OF THEIR ROLE IN APOPTOSIS AS INDUCED BY <i>Polyalthia longifolia</i> (Sonn.) Thwaites LEAF METHANOLIC EXTRACT (PLME) IN HeLa CELL		171
5.1	INTRODUCTION	171
5.1.1	Objectives	172
5.2	MATERIALS AND METHODS	173
5.2.1	Plant Extract Preparation and HeLa Cell Culture	173
5.2.2	HeLa Cell Total Cytoplasmic RNA Isolation	173
5.2.3	Evaluation of Total Cytoplasmic RNA Extracted from HeLa Cells	174
5.2.4	Preparation of Small RNA (smRNA) Library for Deep Sequencing	174
5.2.4(a)	Evaluation of cDNA Library Quality	175

5.2.5	High-Throughput Sequencing	175
5.2.6	High-Throughput Data Analysis	176
5.2.7	Screening and Cluster Analysis of miRNA Expression Profile	179
5.2.8	Meta-Analysis of miRNA Expression Data	179
	5.2.8(a) MiRNA-Gene Interaction Analysis	179
5.2.9	Gene Ontology and Pathway Analysis	181
5.2.10	Pathway Analysis	181
5.3	RESULTS	183
5.3.1	Cytoplasmic RNA Concentration and Purity Analysis	183
	5.3.1(a) RNA Purity Control Using NanoDrop ND-1000	183
	5.3.1(b) Gel Electrophoresis Assessed RNA Integrity	185
	5.3.1(c) Determination of RNA Integrity Number (RIN) Using 2100 Bioanalyzer	187
5.3.2.	Library Quality Assessment	189
	5.3.2(a) Library Size Assessment using Bioanalyzer DNA 1000 Chip	189
	5.3.2(b) Library Quantity Assessment using Illumina qPCR	191
5.3.3	RNA Sequencing Analysis	193
	5.3.3(a) Quality Control of Raw Reads	193
	5.3.3(b) Transcriptome Mapping Analysis	196
5.3.4	Differentially Expressed (DE) miRNAs in Response to PLME	198
	5.3.4(a) Volcano Plot Analysis	198
5.3.5	Dysregulated miRNAs as Induced by PLME Treatment in HeLa Cells	201
	5.3.5(a) PLME up-regulated miRNAs in HeLa Cells	201

5.3.5(b)	PLME Down-Regulated miRNAs in HeLa Cells	201
5.3.5(c)	Heat Map and Dendrogram for Hierarchical Clustering	203
5.3.6	Prediction and Screening of miRNA Target Genes	205
5.3.7	Meta-Analysis of Candidate Target Genes	210
5.3.7(a)	Gene Ontology Annotation of Target Genes	210
5.3.7(b)	Pathway Analysis	223
5.4	DISCUSSION	227
5.4.1	Isolation and Purification of Cytoplasmic RNA from HeLa Cells	227
5.4.1(a)	Preparation of Cytoplasmic RNA	227
5.4.2	Quantitative and Qualitative Assessment of RNA Quality	229
5.4.2(a)	Spectrophotometric Analysis of Purity and RNA Concentration	229
5.4.2(b)	Gel Electrophoresis Based Assessment of RNA Integrity	231
5.4.2(c)	RNA Integrity Analysis Using Agilent 2100 Bioanalyzer	232
5.4.3	High-Throughput Small RNA Sequencing	234
5.4.3(a)	Next Generation Sequencing (NGS) Technology with Illumina Platform	234
5.4.3(b)	cDNA Library Preparation	235
5.4.3(c)	Library Quality Check Analysis	237
5.4.3(d)	Illumina Genome Analyzer Sequencing	238
5.4.3(e)	Analysis of the Small RNA-Seq	242
5.4.3(f)	Quantification of Transcript using MiRDeep2	247
5.4.3(g)	Quantification of Differentially Expressed miRNAs	249

5.4.4	MiRNA Target Prediction	249
5.4.4(a)	Gene Ontology	252
5.4.4(b)	Pathway Analysis	258
5.5	CONCLUSIONS	263
CHAPTER 6.0: CONCLUSIONS AND SUGGESTIONS FOR FUTURE STUDIES		264
6.1	CONCLUSIONS	264
6.2	Future Study Suggestions	267
REFERENCES		270
APPENDICES		
LIST OF PUBLICATIONS		

LIST OF TABLES

		Page
Table 2.1	The influences of phytochemical agents on the expressions and regulations of miRNA found in cancer pathobiology.	29
Table 3.1	Extraction yield in percentage for <i>Polyalthia longifolia</i> methanolic extract (PLME).	52
Table 3.2	Compounds identified in <i>Polyalthia longifolia</i> methanolic extract (PLME) by GC-MS	52
Table 3.3	Cytotoxicity activity of <i>Polyalthia longifolia</i> methanolic extract (PLME) against HeLa and Vero cells with selectivity index.	57
Table 4.1	Expression of apoptotic-related proteins in vehicle control and PLME treated HeLa cells	142
Table 5.1	Summary of small RNA libraries quantity and base pair size.	192
Table 5.2	The number of genes targeted by computational approaches and experimentally validated databases for up-regulated miRNAs induced by <i>Polyalthia longifolia</i> methanolic extract (PLME) in HeLa cell.	206
Table 5.3	The number of genes targeted by computational approaches and experimentally validated databases for down-regulated miRNAs induced by <i>Polyalthia longifolia</i> methanolic extract (PLME) in HeLa cell.	207
Table 5.4	Indicates the GO terms for biological process adapted from DAVID Bioinformatics.	212
Table 5.5	The GO terms for biological process from Enrich database.	215
Table 5.6	Indicates the GO terms for molecular function adapted from DAVID Bioinformatics.	217
Table 5.7	The GO terms for molecular function from Enrich database.	218
Table 5.8	Indicates the GO terms for cellular component adapted from DAVID Bioinformatics.	220
Table 5.9	The GO terms for molecular function from Enrich database.	221

LIST OF FIGURES

	Page
Figure 2.1	The morphological differences between apoptosis and necrosis mechanisms. 13
Figure 2.2	The effect of ROS on DNA chemical alteration that involves purine, pyrimidines and their hydrogen bonding have been explicit clearly. 18
Figure 2.3	Summarising the action of miRNA in nucleus and in cytoplasmic milieu. 21
Figure 2.4	Plant photo of <i>Polyalthia longifolia</i> and its anatomy 38
Figure 3.1	GC-MS chromatogram of <i>Polyalthia longifolia</i> methanolic extract (PLME). 53
Figure 3.2	The cytotoxicity effects of <i>Polyalthia longifolia</i> methanolic extract (PLME) against HeLa cells assessed by MTT assay. 56
Figure 3.3	The cytotoxicity effects of <i>Polyalthia longifolia</i> methanolic extract (PLME) against Vero cells assessed by MTT assay. 56
Figure 3.4	The cytotoxicity effects of <i>Polyalthia longifolia</i> methanolic extract (PLME) against HeLa cells assessed by CyQUANT assay. 57
Figure 4.1	Flow cytometric analysis of Annexin V/PI in HeLa cells which were treated with <i>Polyalthia longifolia</i> methanolic leaf extracts (PLME) at half IC ₅₀ (11.00 µg/mL), IC ₅₀ (22.00 µg/mL) and double IC ₅₀ (44.00 µg/mL) concentrations for 24 h. 115
Figure 4.2	Histogram of quantitative analysis of viable (Q1), early apoptosis (Q4), late apoptosis (Q2) and necrosis (Q1) HeLa cells treated with <i>Polyalthia longifolia</i> methanolic leaf extracts (PLME) at half IC ₅₀ (11.00 µg/mL), IC ₅₀ (22.00 µg/mL) and double IC ₅₀ (44.00 µg/mL) concentration for 24 h. 116
Figure 4.3	Distribution of cell cycle phases in HeLa cells induced by <i>Polyalthia longifolia</i> methanolic leaf extracts (PLME) treatment at half IC ₅₀ (11.00 µg/mL), IC ₅₀ (22.00 µg/mL) and double IC ₅₀ (44.00 µg/mL) concentration for 24 h via propidium iodide based flow cytometry analysis. 120
Figure 4.4	Histogram of quantitative analysis of cell cycle distribution (%) in HeLa cells treated with <i>Polyalthia longifolia</i> methanolic leaf extracts (PLME) at half IC ₅₀ (11.00 µg/mL), IC ₅₀ (22.00 µg/mL), and double IC ₅₀ (44.00 µg/mL) concentration for 24 h. 121

Figure 4.5	Effect on the mitochondrial membrane potential induced by <i>Polyalthia longifolia</i> methanolic leaf extract (PLME) treatment at half IC ₅₀ (11.00 µg/mL), IC ₅₀ (22.00 µg/mL), double IC ₅₀ (44.00 µg/mL) concentration and CCCP for 24 h in HeLa by flow cytometry analysis.	124
Figure 4.6	Mitochondrial membrane potential quantitative analysis for HeLa cells treated with <i>Polyalthia longifolia</i> methanolic leaf extract (PLME) at half IC ₅₀ (11.00 µg/mL), IC ₅₀ (22.00 µg/mL), double IC ₅₀ (44.00 µg/mL) concentration and CCCP for 24 h.	125
Figure 4.7	DCF standard curve utilised for interpreting intracellular ROS generation in <i>Polyalthia longifolia</i> methanolic leaf extract (PLME) treated HeLa cells.	127
Figure 4.8	Reactive oxygen species (ROS) production in (A) HeLa cells treated with <i>Polyalthia longifolia</i> methanolic leaf extract (PLME) at half IC ₅₀ (11.00 µg/mL), IC ₅₀ (22.00 µg/mL), double IC ₅₀ (44.00 µg/mL) concentrations and H ₂ O ₂ for 24 h.	128
Figure 4.9	Image analysis of comet assay by CASP version 1.2.2 software of HeLa cells treated with <i>Polyalthia longifolia</i> methanolic leaf extracts (PLME) at half IC ₅₀ (11.00 µg/mL), IC ₅₀ (22.00 µg/mL) double IC ₅₀ (44.00 µg/mL) concentration for 24 h and H ₂ O ₂ (15 min).	133
Figure 4.10	The generation of comet numbers in HeLa cells treated with <i>Polyalthia longifolia</i> methanolic leaf extracts (PLME) at half IC ₅₀ (11.00 µg/mL), IC ₅₀ (22.00 µg/mL), double IC ₅₀ (44.00 µg/mL) in 24 h and H ₂ O ₂ for 15 min.	136
Figure 4.11	The relative comet tail length of HeLa cells treated with <i>Polyalthia longifolia</i> methanolic leaf extracts (PLME) at half IC ₅₀ (11.00 µg/mL), IC ₅₀ (22.00 µg/mL) double IC ₅₀ (44.00 µg/mL) concentration in 24 h and H ₂ O ₂ (15 min).	136
Figure 4.12	The relative comet tail moment in HeLa cells treated with <i>Polyalthia longifolia</i> methanolic leaf extracts (PLME) at half IC ₅₀ (11.00 µg/mL), IC ₅₀ (22.00 µg/mL) double IC ₅₀ (44.00 µg/mL) concentration in 24 h and H ₂ O ₂ for 15 min.	137
Figure 4.13	The percentages of relative head and tail DNA in HeLa cells treated with <i>Polyalthia longifolia</i> methanolic leaf extracts (PLME) at half IC ₅₀ (11.00 µg/mL), IC ₅₀ (22.00 µg/mL) double IC ₅₀ (44.00 µg/mL) concentration in 24 h and H ₂ O ₂ for 15 min.	137
Figure 4.14	Bovine serum albumin (BSA) protein standard curve from bicinchoninic acid (BCA) protein assay.	139

Figure 4.15	Human apoptosis proteome profile array of HeLa cells treated with <i>Polyalthia longifolia</i> methanolic leaf extracts (PLME) at IC ₅₀ (22.00 µg/mL) concentration for 24 h.	140
Figure 4.16	Histogram of quantitative analysis of apoptotic protein expressions between vehicle control and <i>Polyalthia longifolia</i> methanolic leaf extracts (PLME) treated HeLa cells at IC ₅₀ (22.00 µg/mL) concentration for 24 h (A to I).	141
Figure 5.1	Flow chart of the methodology adopted to identify miRNAs in HeLa cells as induced by <i>Polyalthia longifolia</i> methanolic extract (PLME) at IC ₅₀ concentration (22.00 µg/mL).	177
Figure 5.2	Flow chart of miRDeep2 module.	178
Figure 5.3	NanoDrop ND-1000 results displaying RNA absorbance spectrum of vehicle control (A) and <i>Polyalthia longifolia</i> methanolic extract (PLME) treated HeLa cells (B).	184
Figure 5.4	Agarose gel containing RNA isolated from vehicle control and PLME treated HeLa cells.	186
Figure 5.5	Agilent 2100 Bioanalyzer shows electrophoretic traces for RNA of vehicle control (A) and <i>Polyalthia longifolia</i> methanolic extract (PLME) treated HeLa cells (B).	188
Figure 5.6	Typical results from Agilent 2100 Bioanalyzer electropherogram trace of vehicle control (A) and <i>Polyalthia longifolia</i> methanolic extract (PLME) treated (B) exhibiting evidence of microRNA purified from their respective cDNA libraries.	190
Figure 5.7	Observed C _t values of vehicle control and <i>Polyalthia longifolia</i> methanolic extract PLME treated HeLa cell libraries obtained from qPCR analysis.	192
Figure 5.8	The total read of base pair and total reads generated from vehicle control and <i>Polyalthia longifolia</i> methanolic extract (PLME) treated HeLa cells.	194
Figure 5.9	Box-and-whiskers plot displaying GC and AT content from vehicle control and <i>Polyalthia longifolia</i> methanolic extract (PLME) treated HeLa cells.	194
Figure 5.10	Box-and-whiskers plot exhibiting the Phred Q20 and Q30 quality produced by vehicle control and <i>Polyalthia longifolia</i> methanolic extract (PLME) treated HeLa cells.	195

Figure 5.11	Small RNA sequencing read statistics of the (A) vehicle control and (B) <i>Polyalthia longifolia</i> methanolic extract (PLME) treated HeLa cells.	197
Figure 5.12	Volcano plot displaying differentially expressed miRNA identified by <i>Polyalthia longifolia</i> methanolic extract (PLME) treated HeLa cells.	200
Figure 5.13	Graph bar indicating log ₂ fold change (FC) of the dysregulated miRNA in <i>Polyalthia longifolia</i> methanolic extract (PLME) treated over vehicle control HeLa cells with at least 1000 normalised reads transcript per million (TPM).	202
Figure 5.14	Heat Map and dendrogram represents the hierarchical clustering of the differentially expressed miRNAs (HeLa) based on normalised TPM reads (above 1000 reads).	204
Figure 5.15	Enrich database annotated GO terms for biological process with combinatorial scores.	216
Figure 5.16	Enrich database annotated GO terms for molecular function with combinatorial scores.	219
Figure 5.17	Enrich database annotated GO terms for cellular component with combinatorial scores.	222
Figure 5.18	The chart with inserted table indicates the top 10 ranked pathways identified through KEGG pathway from Enrich database.	224
Figure 5.19	The chart with inserted table indicates the top 10 ranked pathways identified through BIOCARTA pathway from Enrich database.	225
Figure 5.20	The chart with inserted table indicates the top 10 ranked pathways identified through REACTOME pathway from Enrich database.	226
Figure 6.1	Postulated mechanisms by which <i>Polyalthia longifolia</i> methanolic extract (PLME) induce apoptosis in cervical carcinoma HeLa cells.	268

LIST OF PLATES

	Page
Plate 3.1 Vehicle control viable human cervical cancer cells (HeLa) stained with Giemsa observed at (A) magnification of 100X, (B) magnification of 200X and (C) magnification of 400X.	59
Plate 3.2 Morphological changes in human cervical cancer cells (HeLa) treated with <i>Polyalthia longifolia</i> methanolic extract (PLME) at 22.00 µg/mL for 6 h.	60
Plate 3.3 Morphological changes in human cervical cancer cells (HeLa) treated with <i>Polyalthia longifolia</i> methanolic extract (PLME) at 22.00 µg/mL for 12 h.	61
Plate 3.4 Morphological changes in human cervical cancer cells (HeLa) treated with <i>Polyalthia longifolia</i> methanolic extract PLME at 22.00 µg/mL for 24 h.	62
Plate 3.5 Morphological changes in human cervical cancer cells (HeLa) treated with <i>Polyalthia longifolia</i> methanolic extract (PLME) at (22.00 µg/mL) for 36 h.	63
Plate 3.6 Holographic phase contrast images of vehicle control human cervical cancer cells (HeLa) were displayed at the (A) magnification of 200X while image at (B) served as a closer inspection of (A)	65
Plate 3.7 Holographic phase contrast images of morphological alterations induced in human cervical cancer cells (HeLa) by <i>Polyalthia longifolia</i> methanolic extract (PLME) at 22.00 µg/mL in 6 h were displayed at the (A) magnification of 200X while image at (B) served as a closer inspection of (A).	66
Plate 3.8 Holographic phase contrast images of morphological alterations induced in human cervical cancer cells (HeLa) by <i>Polyalthia longifolia</i> methanolic extract (PLME) at 22.00 µg/mL in 12 h at the (A) magnification of 200X while image at (B) served as a closer inspection of (A).	68
Plate 3.9 Holographic phase contrast images of morphological alterations induced in human cervical cancer cells (HeLa) by <i>Polyalthia longifolia</i> methanolic extract (PLME) at 22.00 µg/mL in 24 h at the (A) magnification of 200X while image at (B) served as a closer inspection of (A).	69

Plate 3.10	Holographic phase contrast images of morphological alterations induced in human cervical cancer cells (HeLa) by <i>Polyalthia longifolia</i> methanolic extract (PLME) at 22.00 µg/mL in 36 h at the (A) magnification of 200X while image at (B) served as a closer inspection of (A).	70
Plate 3.11	SEM micrographs demonstrating ultrastructure aspects of vehicle control human cervical cancer cells (HeLa).	73
Plate 3.12	SEM micrographs revealing the changes in ultrastructural characteristics of treated human cervical cancer cells (HeLa) induced by <i>Polyalthia longifolia</i> methanolic extract (PLME) at 22.00 µg/mL in 6 h.	74
Plate 3.13	SEM micrographs revealing the changes in ultrastructural characteristics of treated human cervical cancer cells (HeLa) induced by <i>Polyalthia longifolia</i> methanolic extract (PLME) at 22.00 µg/mL in 12 h.	75
Plate 3.14	SEM micrographs revealing the changes in ultrastructural characteristics of treated human cervical cancer cells (HeLa) induced by <i>Polyalthia longifolia</i> methanolic extract (PLME) at 22.00 µg/mL in 24 h.	76
Plate 3.15	SEM micrographs revealing the changes in ultrastructural characteristics of treated human cervical cancer cells (HeLa) induced by <i>Polyalthia longifolia</i> methanolic extract (PLME) at 22.00 µg/mL in 36 h.	77
Plate 3.16	Higher magnification TEM micrographs of vehicle control human cervical cancer HeLa.	79
Plate 3.17	Higher magnification TEM micrographs of <i>Polyalthia longifolia</i> methanolic extract (PLME) treated in human cervical cancer HeLa cells at 22.00 µg/mL for 6 h .	80
Plate 3.18	Higher magnification TEM micrographs of <i>Polyalthia longifolia</i> methanolic extract (PLME) treated in human cervical cancer HeLa cells at 22.00 µg/mL for 12 h.	81
Plate 3.19	Higher magnification TEM micrographs of <i>Polyalthia longifolia</i> methanolic extract (PLME) treated in human cervical cancer HeLa cells at 22.00 µg/mL for 24 h.	83
Plate 3.20	Higher magnification TEM micrographs of <i>Polyalthia longifolia</i> methanolic extract (PLME) treated in human cervical cancer HeLa cells at 22.00 µg/mL for 36 h.	84
Plate 4.1	Photomicrograph of vehicle control HeLa cells indicating no DNA damage.	130

Plate 4.2	Photomicrograph of <i>Polyalthia longifolia</i> methanolic leaf extract (PLME)-induced DNA damage in HeLa cells treated with half IC_{50} (11.00 $\mu\text{g}/\text{mL}$) for 24 h.	130
Plate 4.3	Photomicrograph of <i>Polyalthia longifolia</i> methanolic leaf extract (PLME)-induced DNA damage in HeLa cells treated with IC_{50} (22.00 $\mu\text{g}/\text{mL}$) for 24 h.	131
Plate 4.4	Photomicrograph of <i>Polyalthia longifolia</i> methanolic leaf extract (PLME)-induced DNA damage in HeLa cells treated with double IC_{50} (44.00 $\mu\text{g}/\text{mL}$) for 24 h.	131
Plate 4.5	Photomicrograph of H_2O_2 -induced DNA damage in HeLa cells	132

LIST OF SYMBOLS AND ABBREVIATIONS

$\Delta\Psi_m$	Mitochondrial membrane potential
a.u	Arbitrary unit
A_{230}	Absorbance at 230 nm
A_{260}	Absorbance at 260 nm
A_{280}	Absorbance at 280 nm
Ago	Argonaute
ANOVA	Analysis of Variance
ATP	Adenosine Triphosphate
AVD	Apoptotic volume decrease
BAD	Bcl-2-Associated Death Promoter
BAX	BCL-2-Associated X Protein
BCA	Bicinchoninic acid assay
BCL-2	B-Cell Lymphoma 2
BCL-w	BCL-2-like protein 2
BIK	BCL-2 interacting killer
BIM	Bcl-2-like protein 11
CCCP	Carbonylcyanide- <i>m</i> -chlorophenylhydrazone
CS	Combinational score
DAVID	Database for Annotation, Visualization and Integrated Discovery
DCF	2', 7'-dichlorodihydrofluorescein
DCFH-DA	2',7'-dichlorodihydrofluorescein diacetate
DE	Differential expression
DMSO	Dimethyl sulfoxide
DMEM	Dulbecco Modified Eagle Medium
e.V	Electronvolt
ER	Endoplasmic reticulum
ES	Enrichment score
ETC	Electron Transport Chain
FACS	Fluorescence-Activated Cell Sorting
FDR	False discovery rate

FC	Fold change
FBS	Fetal Bovine Serum
FITC	Fluorescein isothiocyanate
FSC	Forward scattered light
GC-MS	Gas Chromatography–Mass Spectrometry
GO	Gene Ontology
GRCh38	Genome Reference Consortium Human Build 38
H₂O₂	Hydrogen peroxide
H3K4	Lysine 4 of Histone 3
HDM	Holographic Digital Microscopy
IC₅₀	Inhibition Concentration by half
JC-1	5,5',6,6'-tetrachloro-1,1',3,3'tetraethylbenzimidazolyl-carbocyanine iodide
KEGG	Kyoto Encyclopedia of Genes and Genomes
kV	Kilovolt
LC	Lead citrate
LM	Light Microscope
m.A	Mili Ampere
MAPKs	Mitogen-activated protein kinase
m/z	Mass-to-charge ratio
miRNA	microRNA
NFκB	Nuclear transcription factor kappa B
NGS	Next generation sequencing
NOXA	Phorbol-12-myristate-13-acetate-induced protein 1
P21	Cyclin-dependent kinase inhibitor
P27	Cyclin-dependent kinase inhibitor 1B
P53	Tumor suppressor protein
PBS	Phosphate Buffer Saline
PCR	Polymerase chain reaction
PE	Paired-end
PI	PLME
PS	Phosphatidylserine
PUMA	p53 upregulated modulator of apoptosis

Rb	Retinoblastoma protein
ROS	Reactive oxygen species
SEM	Scanning Electron Microscope
SSC	Side scattered light
TPM	Transcripts per million
UA	Uranyl acetate
UTR	Untranslated Region
Δp	Electrochemical proton motive force
ΔpH_m	Mitochondrial pH gradient

**KAJIAN ASAS MEKANISME TINDAKAN POLIFENOLIK DARIPADA
Polyalthia longifolia (Sonn.) Thwaites DALAM SEL HELA BERKAITAN
DENGAN PENGAWALATURAN MICRORNA**

ABSTRAK

Polyalthia longifolia (Sonn.) Thwaites adalah sejenis tumbuhan pokok malar hijau yang tersohor memiliki faedah perubatan dalam merawat pelbagai penyakit. Sugguhpun faedah etnoperubatan *P. longifolia* telah diiktiraf, namun, kajian mengenai aktiviti antikanser bersifat apoptotik melibatkan microRNAs (miRNA) serta mekanismenya yang tidak pernah dikaji secara terperinci. Oleh itu, kajian ini dilaksanakan untuk mengkaji secara komprehensif tentang ciri-ciri tersebut. Profil Gas Chromatography-Mass spektrometri (GC-MS) PLME telah disediakan. Empat puncak utama melebihi julat kualiti 90% berbanding dengan koleksi data NIST dan Wiley telah dipilih melalui spectrum GC-MS. Ujian sitotoksiti untuk ekstrak PLME telah dijalankan dengan menggunakan ujian-ujian MTT and CyQUANT. Nilai IC₅₀ yang diperoleh adalah sebanyak 22.00 µg/mL dalam masa 24 jam. Pemerhatian dengan menggunakan pelbagai teknik mikroskop mengesahkan bahawa sel-sel HeLa yang dirawat dengan PLME mempamerkan morfologi bagi ciri-ciri apoptosis. Dalam usaha untuk mengesan dan mengukur apoptosis, beberapa cerakin biokimia telah dijalankan dengan merawat sel-sel HeLa dengan kepekatan PLME sebanyak separuh IC₅₀ (11.00 µg/ mL), IC₅₀ (22.00 µg/ mL) dan dua kali IC₅₀ (44.00 µg/ mL). Analisis sitometri aliran dengan pewarnaan Annesin V/PI mengesahkan bahawa ekstrak PLME merangsang apoptosis dalam sel-sel HeLa bersandar kepada kepekatan dos manakala analisis sitometri aliran dengan pewarnaan PI dalam menentukan kitaran sel menunjukkan pengumpulan sel-sel di fasa sub G₀/G₁, G₀/G₁ dan G₂/M. Kajian

analisis sitometri aliran dengan pewarnaan JC-1 pula membuktikan peningkatan penyahkutuban membran mitokondria yang bersandarkan kepada kepekatan ekstrak PLME. Di samping itu, ekstrak PLME turut memberi kesan pada spesies oksigen reaktif intrasel (ROS) dengan mempamerkan aktiviti antioksidan (separuh IC_{50}) dan pro-oksidan (IC_{50} and dua kali IC_{50}) di dalam sel HeLa. Rawatan PLME juga menyebabkan kerosakan DNA sel HeLa bersandarkan kepada kepekatan ekstrak. Tatasusunan profil proteomik menunjukkan kehadiran protein bersifat pro-apoptosis dan anti-apoptosis apabila sel-sel HeLa dirawat dengan ekstrak PLME pada kepekatan IC_{50} . Kajian ini mengandaikan peranan p53 yang menjadi pengantara apoptosis, perencat kitaran sel dan menyebabkan penyahkutuban potensial membran mitokondria dengan modulasi status redoks dalam sel HeLa. Sel-sel HeLa yang telah dirawat dengan ekstrak PLME memperlihatkan pengekspresan miRNA yang menurun terutamanya bagi miR-331-3p, miR-125a-5p, miR-125b-5p, miR-34a-5p, miR-193b-3p, miR-193a-5p, miR-186-5p, miR-370-3p, let-7i-3p, miR-222-3p, miR-296-5p, miR-15b-5p, miR-361-5p dan miR-484. Kesemua 14 miRNA ini telah digunakan untuk ramalan sasaran gen melalui kaedah analisis berkomputer yang mewajarkan fungsi anotasi miRNA ini dengan aktiviti apoptosis. Kesimpulannya, keputusan yang diperolehi daripada kajian ini membuktikan kepentingan PLME sebagai calon terapeutik dalam memengaruhi apoptosis melalui pengawalaturan miRNAs dalam sel HeLa.

**FUNDAMENTAL STUDIES ON THE MECHANISM OF *Polyalthia longifolia*
(Sonn.) Thwaites POLYPHENOLS ACTION IN HELA CELLS IN RELATION
TO MICRORNA REGULATION**

ABSTRACT

Polyalthia longifolia (Sonn.) Thwaites is a lofty, evergreen tree that extensively known for its medicinal beneficial in treating various ailments. Though *P. longifolia* ethnomedicinal benefits had been recognised, studies concerning its anticancer and apoptotic cell death activity in relation to microRNAs (miRNA) and their mechanism had never been studied in detail. Herein, this study was conducted to comprehensively study these characteristics. The PLME GC-MS profile was prepared. Four major peaks with the quality range above 90 in reference to NIST and Wiley libraries were determined in the GC-MS spectra. The cytotoxicity effect of PLME was investigated using (3-(4,5-dimethylthiazol-2-yl)-2,5-diphenyl tetrazolium bromide) MTT and CyQUANT assays against HeLa cells. The IC₅₀ value was quantified as 22.00 µg/mL at 24 h. Different microscopy techniques were implemented and the observations obtained affirmed that PLME treated HeLa cells exhibiting marked morphological features to apoptosis characteristics. In order to detect and quantify the apoptosis, various biochemical assays were conducted with half IC₅₀ (11.00 µg/mL), IC₅₀ (22.00 µg/mL) and double IC₅₀ (44.00 µg/mL) concentrations of PLME treated in HeLa cells. The Annexin V/PI flow cytometry analysis showed that PLME induces apoptosis in HeLa cells in dose-dependent manner whereas the PI flow cytometric analysis for cell cycle demonstrated the accumulation of cells at sub G₀/G₁, G₀/G₁ and G₂/M phases. Investigation with JC-1 flow cytometry analysis indicated increase in mitochondria membrane potential

depolarisation corresponding to increase in PLME concentrations. PLME was also shown to influence intracellular reactive oxygen species (ROS) by exerting anti-oxidant (half IC_{50}) and pro-oxidant (IC_{50} and double IC_{50}) effect against HeLa cells. PLME treatment also displayed DNA damage in HeLa cells in concentration depended fashion. The proteomic profiling array exposed the expression of pro-apoptotic and anti-apoptotic proteins upon PLME treatment at IC_{50} concentration in HeLa cells. This study postulated the role of p53 into mediating apoptosis, cell cycle arrest and mitochondrial potential depolarisation by modulating the redox status of HeLa cells. PLME treated HeLa cells expressed higher numbers of down-regulated miRNAs particularly miR-331-3p, miR-125a-5p, miR-125b-5p, miR-34a-5p, miR-193b-3p, miR-193a-5p, miR-186-5p, miR-370-3p, let-7i-3p, miR-222-3p, miR-296-5p, miR-15b-5p, miR-361-5p and miR-484. These 14 miRNAs were then used for gene target prediction through analytical computational methods which justified their functional annotation to apoptosis activity. In conclusion, it was proven the importance of PLME as therapeutic candidate in exerting apoptosis through the regulation of miRNAs in HeLa cell.

CHAPTER 1.0: INTRODUCTION

1.1 Overview and Rationale of Study

Cervical cancer persists to be a major health enigma despite much preventive enhancement comprising of screening and vaccination gestated since early 1970's. This malignant neoplasm, eventuates when the circumambient cells of cervix region unexpectedly conduce to abnormal growth of cells. With the estimation of 528, 000 cases every year, cervical cancer ranks as the fourth most common mortality in the world with the largest number of incidences sprouting from poor classes and rural areas (Singh *et al.*, 2011; NCI, 2014). In reference to Malaysian National Cancer Registry (2016), as from year 2007 till 2011, a total of 7.7% of cervical cancer cases were collectively reported and considered high compared to several other Asian and Western countries. Enumerating the prevalent cases of cervical cancer, WHO (2014) and Global Cancer Incidence, Mortality and Prevalence (GLOBAICON) estimated 4696 of annual cases in Malaysia alone (Zaridah, 2014).

Several effective cervical cancer drugs have been making room in the market; cisplatin, cyclophosphamide, ifosfamide, doxorubicin, bleomycin and neomycin, yet up till now, prominent drawbacks still engender inept results (Guoliu, 2014). When patients at early stages endure surgery, infertility befalls the younger ones while others simply sustain relapse due to pertinacious, revertive and metastatic competency of cancer (Yaoxian *et al.*, 2013). An overall of 70% patients manifested relapse by undergoing primary surgery and radiotherapy to encounter nodal metastases and more localized tumors, however 10% - 20% relapse still occur without the involvement of lymph node (Friedlander and Grogan, 2002). This collateral aspect is attributed to acquired drug resistancy during treatment of cancer. The tumors tend to capitulate during early treatment seeking deliberate procuring

mutations as part of adaptive measurements to counterattack therapeutic drugs' targets and signaling pathways (Longley and Johnston, 2005). Tumors have a tendency of high degree molecular heterogeneity that only manifest during therapy induction. These subpopulation cells commencing from the original tumor, retaliate against anti-cancer drugs by means of selection based resistancy (Swanton, 2012). A combined treatment of chemotherapy and radiation (concurrent chemoradiation) is delivered contemporaneously as main treatment, though adverse effects were perceived corroding bone marrow and nervous system, while increasing the danger to infection susceptibility due to loss of white blood cells (ACS, 2015).

At present, considerable models of cervix carcinoma have been actualize with different cell lines and this investigation contemplated HeLa cells in regard to its congruous representation of cervical cancer model. HeLa cells are the very first human cells to be cultured of neoplastic cell line deriving from the cervical carcinoma of a woman back in 1951 (Scherer *et al.*, 1953). A number of preceding works implicated on human sensitivity (Batts, 2010), radiation and toxic substances effect had substantiated the key features of HeLa cells of being durable and prolific (Smith, 2002). This cancerous cell line displays several basic fundamental characteristics similar to normal cells in the course of protein/gene expression, cell signaling, proliferation and regulation. Moreover, HeLa cells are also prone to infections making them a perfect subject to study numerous cell culture features, taking into account bacteria, hormones, drugs, proteins and viruses (Masters, 2002).

The practice of integrating modernized genomics, proteomics and functional analytical approaches have intensified the aptitude of novel genes discovery and signaling pathways concerning the relationship between tumor cells and specific drug treatment (Holohan, 2013). A diverse range of molecular mechanisms have

been implicated in drug resistancy which may include the association of microRNA. MicroRNAs (miRNAs) have up-surged in recent past as a new class of small evolutionarily conserved non-coding RNAs that negatively regulate gene expression (Cannell *et al.*, 2008; Sun *et al.*, 2008; Bartel, 2009). These miRNAs mature into 18 to 25 long nucleotides that arrest target genes by influencing translation and/or stability of mRNA through partial complementary binding to their mRNA region of 3'UTR and 5'UTR (Lytle, *et al.*, 2007). Comparatively, 35828 mature miRNA products from 223 species have been published up to date (database reviewed in October 2016) in miRBase (ver.21), a continuous and well maintained database (Kozomara and Griffiths-Jones, 2014). The functions of miRNAs extends from perpetrating heterochrony, cell differentiation, cell proliferation, cell death, metabolic control, transposon silencing to antiviral defense in cells (Kim *et al.*, 2009). The capability of miRNA to regulate cell functions at transcriptional and post-transcriptional levels anticipated a whole new cutting edge for therapeutic strategies.

The very first anti- cancer drug was discovered of synthetic origin established upon the so-called nitrogen mustard (an acylating agent that mutates DNA helicase) resort to operate as blister gas during World War I. In the wake of World War II, preliminary exploration of microbial world offered an even better opening to a significant number of microbial products with antibiotic activity against eukaryotic cells, notably mammals. There were also few observations concerning plant secondary metabolites displaying activity against tumor cells, hence the worldwide preceding works from early 1950's till date to ferret out plant products for their hidden antidote as antitumor agents (Newman, 2005).

Current literatures suggests nature as a reservoir for multi-targeting phytochemicals that may possess the key to eliminate cancer (Kong and Yu, 2016;

Saxena *et al.*, 2016). Phytochemicals for example resveratrol, (–)-epigallocatechin gallate (EGCG) and myricetin had been reported to instigate diverse molecular signal transduction pathways where research progressions focused upon on their effects in cancer cell death or cancer growth inhibition (Jung *et al.*, 2010; Shim *et al.*, 2008; Zykova *et al.*, 2008). In the present study, *Polyalthia longifolia* is discussed of its cytotoxicity and alterations to HeLa cells contributing to an overview of how its crude extract reacts on specific molecular and cellular targets in order to assert its anti-cancer affects. The overall strategy of using *P. longifolia* not only discovers the many target aspects but also aids for a target- based approach on the basis of data impeccably obtained from small RNAs (microRNA) distribution. This study is presented in the purpose of expanding the level of knowledge concerning the aptitude of *P. longifolia* crude extract as a chemopreventive agent through an understanding of its mechanism of action and at the level of miRNA regulation.

1.2 Objectives

The current study was undertaken with the following objectives:

- 1) To determine *in vitro* cytotoxic activity of methanolic leaf extract of *P. longifolia* (PLME) on HeLa cells.
- 2) To demonstrate the mode of action by which PLME exerts in HeLa cells through different microscopic techniques.
- 3) To assess the mechanism of cell death in HeLa cells treated with PLME.
- 4) To identify the profusely induced miRNA(s) as the outcome of PLME on HeLa cells.
- 5) To study the roles of dysregulated miRNA(s) by *in silico* and meta-analytic approaches concerning gene interactions, functions and pathway analysis for PLME treated HeLa cells.

CHAPTER 2.0: LITERATURE REVIEW

2.1 Apoptosis

Apoptosis is a term adopted from the Greek, denoting “dropping off”, an adumbration likely to the falling of leaves from trees in autumn. The word received its great endurance when Kerr *et al.* (1972) recount the plight upon which a cell is initiated by a number of stimuli in directing itself in pursue of death.

Apoptosis is an indicative of a number of morphological changes that witness cell shrinkage, membrane blebbing, nuclear fragmentation and chromatin condensation (Wyllie *et al.*, 1980; Kerr *et al.*, 1994). Even though this apoptosis is extremely coordinated, still, its role in both physiology and pathology, is subtly controvertible (Merkle, 2009; Mohan, 2010), for an instance, the genetic regulators for apoptosis if disrupted by mutation becomes a great contributor to a number of human diseases stretching from neurodegenerative disorders to cancers (Thompson, 1995).

2.1.1 Morphological Changes in Apoptosis

In despite of cell type and species, the cellular structure alterations pertaining to nucleus and cytoplasm regions are astonishingly comparable and similar during apoptosis (Hacker, 2000; Saraste and Pulkki, 2000). Often enough, the cells arrives to its final state of cellular fragmentation, several hours after the commencement of programmed cell death, yet the time taken is contingent upon cell type, stimulus and apoptotic pathway as described in Figure 2.1 (Ziegler and Groscurth, 2001).

During apoptosis, the cells contract to appear round in shape, followed by decrement in cellular volume and the withdrawal of pseudopods. Subsequent alteration will beget in the nucleus uncovering chromatin condensation and nuclear

fragmentation, the very hallmark of apoptotic morphology occurring in nucleus (Hanahan and Weinberg, 2000; Galuzzi *et al.*, 2007).

The chromatin condenses around the membrane circumference of the nucleus, generally resembling a crescent or ring-like structure. Typically, the chromatin thickens to the point where it ruptures within the confinement of the cell membrane, a prevailing feature known as karyorrhexis (Manjo and Joris, 1995). The plasma membrane will remain integral at every point of apoptosis event.

Shortly, the last phase of apoptosis divulges its vulnerability to membrane blebbing, cellular ultrastructure alteration and loss in membrane integrity (Hanahan and Weinberg, 2000; Galuzzi *et al.*, 2007). Given the normal physiology, the apoptotic cells will be engulfed by phagocytic cells (macrophages and neutrophils) before the occurrence of apoptotic bodies.

The artificial cell culture environment, conversely do not facilitate the remnants of apoptotic cells to be phagocytosed, thereby perceives the disintegration of apoptotic cells into necrosis-like state, a condition defined as secondary necrosis (Ziegler and Groscurth, 2001).

2.1.2 Biochemical Changes in Apoptosis

There are three conspicuous biochemical modifications transpiring in apoptosis: 1) caspase activation 2) DNA and protein degradation and 3) membrane alteration and phagocytic cells recognition (Kumar *et al.*, 2010). Naturally, an antecedent of apoptosis is imputed to the eversion of phosphatidylserine (PS) from the inner layer to the outer layer of cell membrane. This expedites the initiation of phagocytosis recognition without the involvement of pro-inflammatory cellular components (Hengartner, 2000).

Thereafter, DNA is degraded into large 50 to 300 kilobase pieces, followed by actions from endonucleases to further disintegrate these DNA into oligonucleosomes in multiples of 180 to 200 base pairs. Though this a distinctive feature of apoptosis, a simple test of DNA ladder in gel electrophoresis might not represent the best outcome, as necrotic cells shares the same consequence of DNA fragmentation too (McCarthy and Evan, 1998).

The enzyme caspase is another addition to apoptosis features upon where the alphabet “c” from the word caspase indicates cystein protease while the “aspase” refers to the enzymes capability to cleave after aspartic acid residues (Kumar *et al.*, 2010). Caspases which are triggered to an active state will drift to excise fundamental elements such as proteins, nuclear scaffold, cytoskeleton and even prompt DNase to accelerate nuclear DNA degradation (Lavrik *et al.*, 2005).

It is to be highlighted that, biochemical analyses of DNA fragmentation and caspase activation should not be solely contemplated as apoptosis, as these signs are capable of eventuating without the favour of caspase or oligonucleosomal DNA fragmentation (Galluzi *et al.*, 2007). The Nomenclature Committee on Cell Death (NCCD) recommended that categorizing of cell death procedures should be based upon morphology criteria alone due to existing vague equivalence between ultrastructure changes and biochemical cell death analyses (Galluzi *et al.*, 2012).

2.2 Apoptosis Detection Method

2.2.1 Detection of Apoptosis through Morphological Analysis

Apoptosis has earned disparate methods to uncover their discrete appearance in cells and one of the most advantageous methods is via electron microscopy observation. The finest revelation of apoptosis within the array of tissues and physiological state

has been construed with the help of investigations carried out by Kerr *et al.* (1972) and Wyllie *et al.* (1980).

The parameter of cell death following treatment with definite drugs every so often marks the experimental endpoint and while apoptotic morphology is concerned; transmission and scanning electron microscope seems requisite. The samples are fixed using osmium tetroxide before being inserted into tiny resins. The resins containing samples are then sliced into ultra thin segments only to be finally stained with uranyl acetate (UA) and lead citrate (LC) prior to transmission electron microscope analysis.

UA delivers the highest electron density with better image and contrast by fastening itself to proteins, ribosomes, membranes, lipids and nucleic acids. The LC however augments the contrasting effects across ribosomes, lipid membranes, cytoskeleton and cytoplasmic compartments. Hence, the LC staining is employed soon after UA (Pandithage, 2013).

Scanning electron microscopy has also been used to examine apoptotic cells. Their characteristic rounded-up phenotype is well represented by this imaging modality (Wyllie *et al.*, 1980; Germain *et al.*, 2007).

Apoptosis can be distinguished via Giemsa stain, in reference to cellular morphology. Giemsa, an interfusion of mythelene blue, eosin and Azure B, trails after DNA phosphate groups to find itself adhesive to adenine-thymine rich DNA region (Damsgaard *et al.*, 1997). The periphery of plasma membrane and the nucleic region are more flawlessly observable through light microscope (Ulukaya *et al.*, 2011).

The HoloMonitor, a quantitative phase contrast microscope is a method modelled to compute the phase shift of live cells or apoptotic cells in their habitual

culture vessel. This is considered as an excellent method since these cells are not perturbed by trypsin or stained for their features to be visible. The microscope devises a phase shift image of cells corresponding to measured phase shift giving away coloured images that respond congruously with the height and thickness of cells (Kemmler *et al.*, 2007).

2.2.2 Detection of Apoptosis via Flow Cytometry Analysis

Flow cytometry is an instrument discovery of laser-based and biophysical technology that can detect cells in a stream of fluid when they pass by an electronic detection apparatus. It exposes multi-parametric analysis pertaining to the physical and chemical properties of apoptotic features in cells (Ornatsky *et al.*, 2010).

The emanation of fluorochromes such as Annexin V-FITC and propidium iodide (PI) facilitates the accuracy of the cell detection. The dye PI binds by interpolating between DNA or RNA bases and once fixing itself to nucleic acids, its fluorescence impels to enhance up 20 to 30 fold (Suzuki *et al.*, 1997). The Annexin V labelled in association of FITC (fluorescent substance) bounds to phosphatidylserine (PS). PS, a membrane positioned under natural circumstance lies within the cytoplasmic milieu of typical cells but gets everted to the cell outer surface upon apoptosis. The displacement of PS extricates the visualization of apoptosis apart from non-apoptotic cells (Vermes *et al.*, 1995; McCarthy and Evan, 1998; Li *et al.*, 2011).

Nevertheless, this technique is not only pertinent for apoptotic cells, but also applicatory for the determination of necrotic cells in the interest of Annexin V binding to PS from the inside of damaged cell membranes of necrotic cells. (Saikumar *et al.*, 1999). A double staining has been proposed to serve the intention of discriminating apoptotic from the necrotic ones. Both Annexin V and PI will be

introduced to the mixture of heterogeneous cells, as a result, apoptotic cells will be stained by Annexin V, while necrotic cells will promote dual staining of Annexin V and PI (Brush, 2000).

2.2.3 The Usage of Flow Cytometry in Cell Quantification

The flow cytometry implements a biophysical technology based on laser and impedance which is utilised completely to quantify individual cells while classifying them in accordance to their biological markers. The cells are first mixed together in a liquid which is then channelled directly into an apparatus that electronically recognises them. Here, thousands of cells are sorted in regard to their physical and chemical properties per second permitting concurrent multi-parametric analysis.

A flow cytometry's function is analogue to a microscope. Instead of producing observable images, the flow cytometry generates automated measurable parameters for large number of cells. The cytometry is composed of five major constituent; (1) a flow cell that arranges cells into a single line to stream across a light beam, (2) the light beam contributes as a sensing device comprised of optical lamps and lasers, (3) a detector that converts the measurement into forward scattered light (FSC) and side-scattered light (SSC), (4) a system amplifier which amplifies the extend of signal mechanical qualities and (5) a computer that serves for interpretation of signal analysis (Nunez, 2001).

The data perceiving technique from flow cytometer is referred to as 'acquisition' and is facilitated with the use of a computer and software that ensures the accuracy of the data (Bakalar and Tomas, 2016). The data received is scaled and converted into single or two dimensional dot plots where the distribution of the dots are sorted on the basis of fluorescence intensity and separated into subsets (defined as gates). The plots are represented on logarithmic scales to avoid overlapping

spectra emission caused by the presence of two or more dyes and also signals received from the detector is subjected to compensation prior to analysis (Bakalar and Tomas, 2016).

The study herein incorporated analysis performed using the fluorescence-activated cell sorting (FACS), an advanced technology deriving from flow cytometry. The technique employed in FACS not only similar to the flow cytometry but is also enhanced in terms of obtaining data in much faster and accurate manner (Julius *et al.*, 1972).

2.2.4 Detection of Apoptosis via Mitochondrial Membrane Potential ($\Delta\Psi_m$)

Apoptotic stimulability is a key lead to $\Delta\Psi_m$ abatement (Zamzami *et al.*, 1995; Scarlett *et al.*, 2000; Gottlieb *et al.*, 2003) that may ensue during oxidizable substrate deficiency in mitochondria, respiration obstruction or inner membrane uncoupling (Halestrap, 1989; Bernardi *et al.*, 2001). The mitochondrion houses a set of proteins that participate throughout the apoptotic mechanism; caspases and cytochrome *c*. The caspases fit in as members of cysteine proteases family, the focal point inducement of several apoptosis processes (Alnemri *et al.*, 1996; Wang, 2001), while emancipation of cytochrome *c* from the intermembrane space into the cytoplasm actuate downstream caspases through apoptosome incitation (Hengartner, 2000; Adrain and Martin, 2001).

The establishment of a recent flow cytometry technique in computing $\Delta\Psi_m$ together with the employment of fluorescent lipophilic substrates connotes apoptosis. The healthy cells uptake these lipophilic molecules to constitute agglomerates that emits bright red fluorescence. On the other hand, apoptotic cells, liberates the lipophilic molecules back into cytoplasmic region due to reduced $\Delta\Psi_m$, giving out green fluorescence, the very outcome of monomeric molecules (Brush, 2000).

2.3 Necrosis

In the beginning, the term necrosis was thought to be the last stage of irrevocable tissue impairment, engaging only upon cells that have already died (Majno and Joris, 1995). Efficaciously over the years, the definition of necrosis has ameliorated to a passive form of cell death unlike apoptosis, but rather accidental without the perceptibility of convoluted regulative mechanisms. Factors such as heat stress or toxic agents are capable of impelling necrotic cell death as well as in many ways provoke apoptotic cell death (Majno and Joris, 1995; Shimizu *et al.*, 1996). The deciding dynamics concerning the fate as either apoptosis or necrosis relies upon the degree of injury and the level of energy within a cell. Altered or reduced ATP generations often shove cell death in the direction of necrosis (Nicotera *et al.*, 1998; Leist and Jaattela, 2001).

Necrosis appears to be a set of distinguished characteristics affecting the morphology of these dying cells as illustrated as in Figure 2.1. The initial response to necrosis is placed contingent on the cell membrane that emerges permeable; as a result, organelles appear dilated while endoplasmic reticulum loses its ribosome. Chromatin condensation only arises in certain cases and nucleus fragmentation occurs late during the stage. Pyknosis and nuclei disintegration are not typical features eventuating in necrotic cell death. Nonetheless, the outflow of hydrolytic enzymes and other cellular components elicit massive inflammation on adjacent cells and tissue.

There are two different forms of necrotic cell death classified mainly on the morphology and participation of lysosomes; autophagic and non-lysosomal degeneration (Clarke, 1990). The autophagic cell death is peculiarized with distinctive nature of vacuoles filled with cellular traces bountifully scattered within

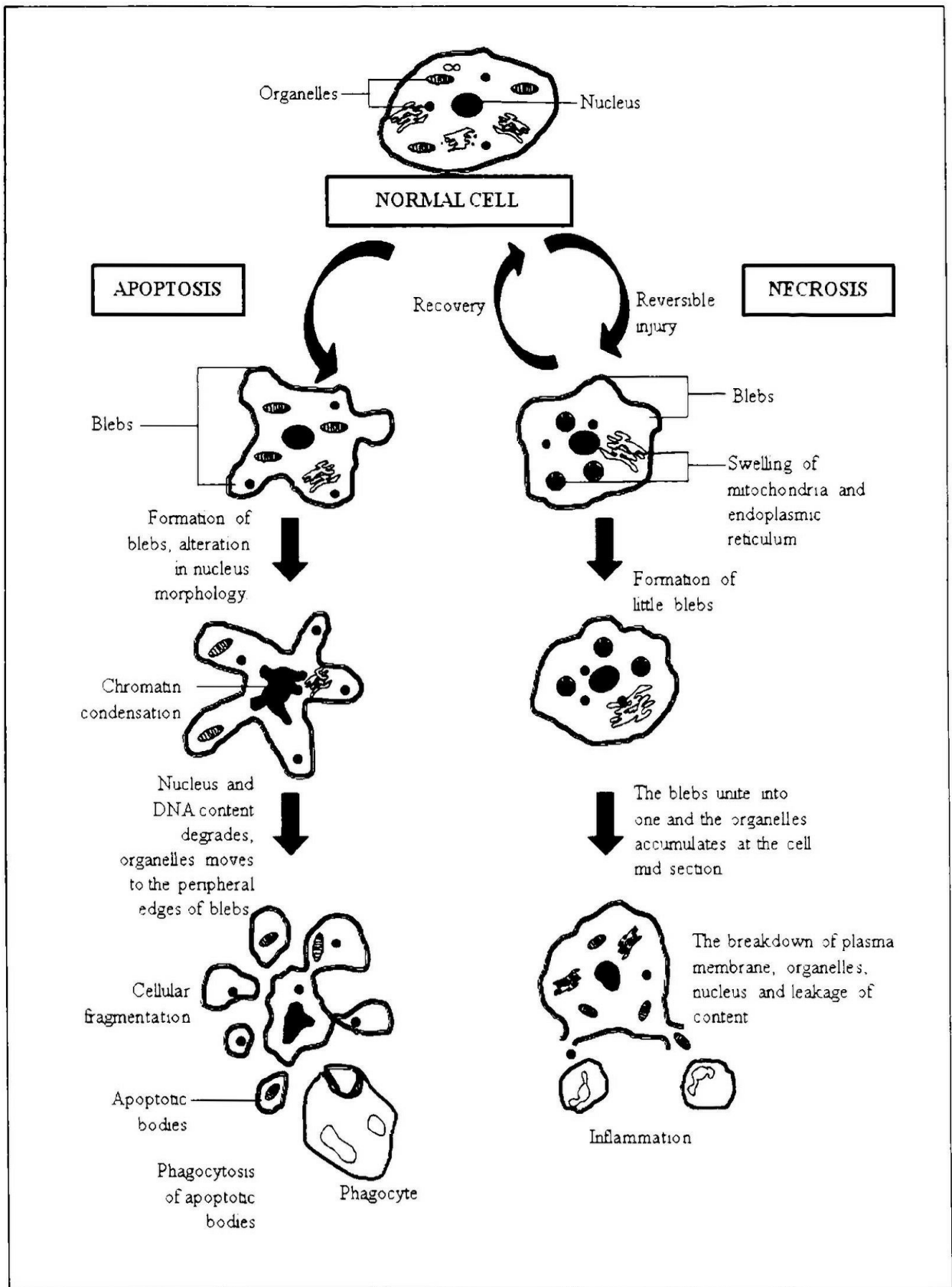


Figure 2.1: The morphological differences between apoptosis and necrosis mechanisms. (Adapted with modification from Rachita, 2014).

the cytoplasm region while the non-lysosomal cell death exhibits unequivocal dilation of organelles, empty spaces formation without the involvement of lysosomes. Apprehending the fact that dying necrotic cells develop higher membrane permeability at the earliest stage, as opposed to apoptosis, researchers had ferret out a technique to detect them.

Due to the mitigated membrane permeability, tiny charged molecules that generally excluded by the cell membrane will then be directed into the cell. The cell will then uptake PI, mono- or dimeric cyanine nucleic acid dyes, such as YOPRO-1, upon where these dyes have greater affinity towards DNA and RNA, hence a suitable correlation was able to uncover between the bounded dye and the outcome of their fluorescence intensity (Kressel and Grouscurth, 1994).

2.4 Cell Cycle

The cell cycle machinery incorporates a set of events that is applied conscientiously during cell replication. Eukaryotes submit to homeostatic balance between the process of cell death and cell proliferation to sustain the intricate network of tissues while acclimating to changing environmental conditions.

With the intention of achieving a balance, there must be a certain linkage uniting cell cycle and programmed cell death together through a controlling set of components (King and Cidlowski, 1995).

2.4.1 Cell Cycle and Apoptosis

Cell cycle is a comprehensive study of four phases; G1 phase, S phase, G2 phase and the final M phase. Genetic materials are conveyed from one cell to another cell and this event necessitates genetic materials to be duplicated in the course of S phase, while the M phase governs the explicit formation of two daughter cells. Both phases

are unequivocally imperative for the identical regeneration of a cell without genetic defectiveness. The cell cycle machinery is as such that M phase ensues only upon the completion of S phase. There are two prefatory phases existing between S and M phases.

The G1 phase is positioned before the S phase while the G2 phase stands in between S and M phase. Differentiating cells often egress away from G1 phase into a dormant state, represented as G0 phase (MacLachlan *et al.*, 1995). The regulation of cell cycle is mediated by two substantial proteins, namely the cyclin (A, B, D, E) and cyclin dependent kinases (cdks). These proteins have to comply with each other through phosphorylation to establish cyclin cdk complexes. When the concentration of these complexes becomes commensurable, the checkpoints endorse the cell to move forward into the subsequent phase.

The cell cycle will come to a halt if the concentration as well as the complexes activity were to perturb, for example, by silencing these complexes, the cell cycle ceases and imparts apoptosis. Additionally, there are also other proteins: p53 and Rb proteins that possess underlying roles in the cell cycle regulation. The p53 protein is coded by p53 tumor suppressor gene, which takes control upon the recognition of DNA impairment during c-radiation or chemotherapy (Kamesaki, 1998; Mathieu *et al.*, 1999). The p53 works by triggering the expression of p21 gene which sequentially arrests the progression of cell cycle by blocking the performance of cyclin cdk complexes. At higher concentration of p53, initiation of BAX transcripts takes place eventuating in apoptosis induction (Kamesaki, 1998). The proto-oncogene c-myc also impacts the cell division by eliciting p53 dependent apoptosis in murine embryonic fibroblast, a good indication of possible link between p53, c-myc and mitochondrial system (Soeng *et al.*, 1999).

The retinoblastoma (Rb) protein, a tumor suppressor comparably binds to specific numbers of transcription factors to inhibit DNA replication while in another stance, the cyclin cdk complexes simply phosphorylates these proteins freeing Rb from the transcription factors, ensuing the cell to proceed into subsequent phase (Evan *et al.*, 1995).

2.5 Reactive Oxygen Species (ROS)

Cancer cells are reputable for mitochondrial dysfunction, high cellular receptor signalling, elevated metabolic, proxisome, oncogene, oxidases, cyclo-oxygenases, lipoxigenases and thymidine phosphorylase activity (Weinberg, 1996; Sugimura, 1998; Halliwell, 1999).

The system of a typical aerobic organism expels reactive oxygen species (ROS) as consequence of oxidative phosphorylation, which can be recognised as hydroxyl radicals ($\cdot\text{OH}$), superoxide anions ($\text{O}_2\cdot^-$), singlet oxygen ($^1\text{O}_2$) and hydrogen peroxide (H_2O_2). The electron transport chain found along the inner membrane of mitochondria accommodates five major protein complexes known as complexes (I, II, III, IV) and ATP synthase. Nearly 80% of superoxide formed at complexes I and III are liberated into the intermembrane space while another 20% are released into the mitochondrial matrix (Buechter, 1988). The transition pores positioned on mitochondria usually facilitates molecular exchanges and at the same time discharges these superoxides into cell's cytoplasm milieu (Scandalios, 2002; Klein and Ackerman, 2003). These superoxides eventually become converted into H_2O_2 that act as secondary messengers with a higher permeability towards any cellular membranes (Nohl *et al.*, 2003).

Customarily, the injurious effects caused by superoxide require abrogative action by antioxidant. However, when the level of superoxide exceeds antioxidants,

the disproportion caused derives to a state known as oxidative stress. The endurance of oxidative stress induces deterioration at the molecular level which also encompasses genomic damage accumulation, altered signalling transduction, gene expression to mitogenesis, transformation, mutagenesis and cell death (Wiseman and Halliwell, 1996; Marshall *et al.*, 1997). This may also lead additionally into an accretion of oncogenic mutations that is implicated in cancer pathogenesis and tumor progression. The diagram from Figure 2.2 explicates the effect of chemical alteration on DNA that involves purine, pyrimidines and their hydrogen bonding that subsequently impinge upon DNA replication. Adversely, oxidative impairment to protease and local tissues instigate tumour growth and metastasis.

2.5.1 Reactive Oxygen Species (ROS) and Cancer

ROS has been extensively inferred in both apoptosis and cancer mechanisms. The intermediate proteins found in apoptosis pathways prompt intracellular generation of ROS to which their deleterious actions are conversely neutralised by the presence of antioxidants. Supposing the ROS mechanism had been attributed to the debatable status of redox and or hydrogen peroxide, both determinants is still accepted as imperative principles (Rollet-Labelle *et al.*, 1998; Tanaka *et al.*, 1998).

Immensely, the commencement of tumorigenesis resolutely catenated to oxidative injuries and as such 8-oxo-2'-deoxyguanosine, an outcome of DNA oxidative component (Mills *et al.*, 1998), had been observed to be extremely mutagenic (Floyd, 1990). The intrusive nature of ROS were observed in several studies notably the signal cascade systems together with activated protein-1 (AP-1), phospholipase A2, nuclear transcription factor kappa B (NFκB), mitogen-activated protein kinase (MAPKs) and c-JUN kinase (Guyton *et al.*, 1996; Bae *et al.*, 1997; Manna *et al.*, 1998; Musonda and Chipman, 1998).

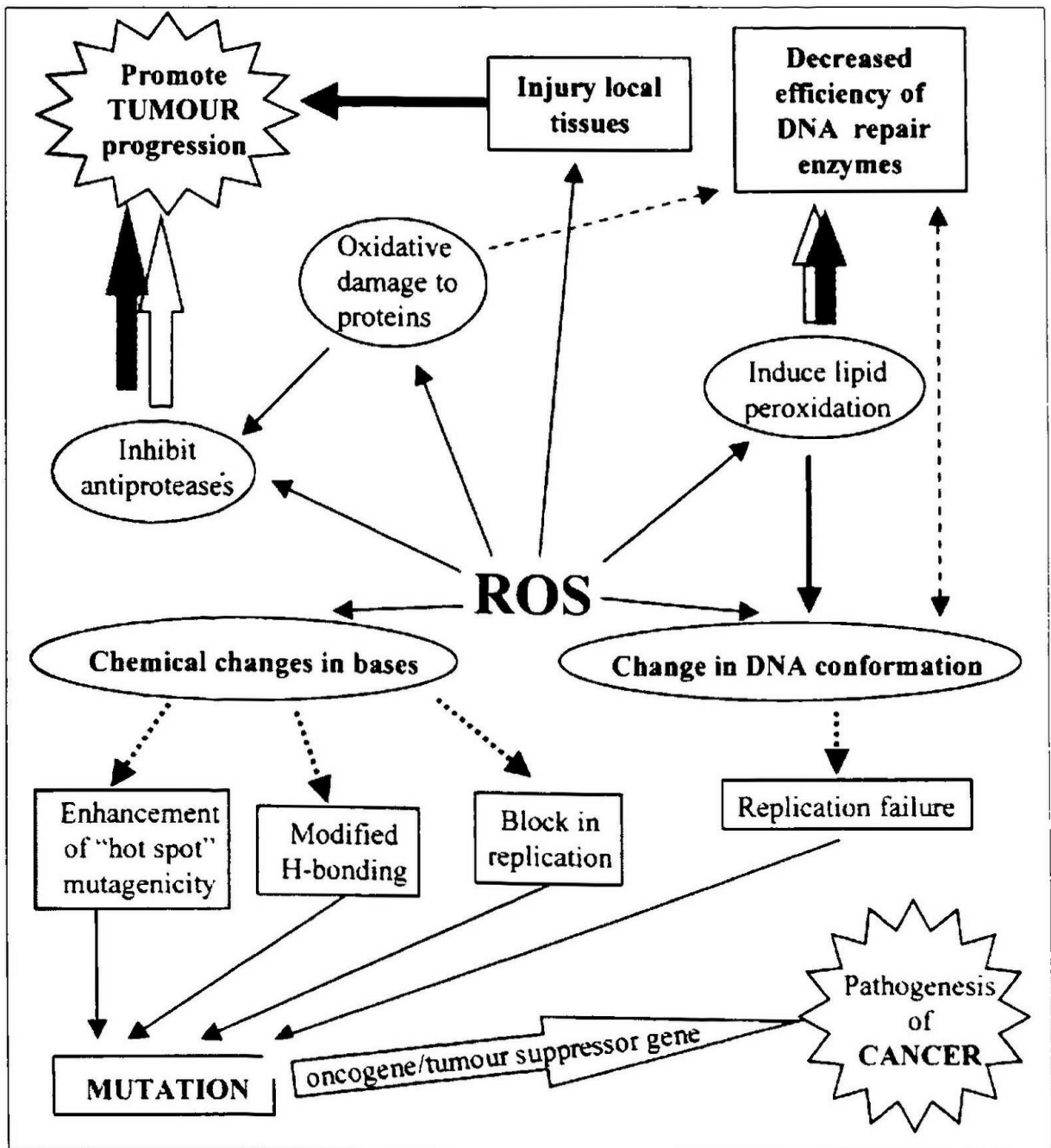


Figure 2.2: The effect of ROS on DNA chemical alteration that involves purine, pyrimidines and their hydrogen bonding have been explicit clearly. The alterations subsequently impinge upon DNA replication while oxidative impairment to protease and local tissues instigate tumour growth and metastasis. (Adapted from Matés and Sánchez-Jiménez, 1999).

To counterbalance this redox reaction, cells work swiftly utilizing a vast platform of biological feedback with the incorporation of cell-cycle growth arrest, gene transcription, induction of signal transduction pathways and DNA damage repairs. These occurrences will then decide the fate of the cell as of necrosis, senescence, apoptosis, or to resist, survive and proliferate (Limoli *et al.*, 1998).

2.6 MicroRNA

The gene expressed microRNAs (miRNAs) have emerged recently as a new class of small evolutionarily conserved non-coding RNAs that negatively regulate gene expression (Cannell *et al.*, 2008; Sun *et al.*, 2008; Bartel, 2009). MiRNAs are a class of non-coding RNAs, 18 to 25 nucleotide long that inhibit the expression of target genes by affecting the translation and/or stability of mRNA by binding to their target sites in the 3'UTR and 5'UTR of the mRNA (Lytle *et al.*, 2007).

These minuscule miRNAs (~21-23 nt) perpetrate heterochrony, cell differentiation, cell proliferation, cell death, metabolic control, transposon silencing and anti-viral defence in cells (Kim *et al.*, 2009; Kozomara and Griffiths-Jones, 2011). MicroRNAs regulate cell function both at transcriptional and post-transcriptional levels which open up a new area of research and play an emerging role in the identification of new therapeutic strategies.

Endogenous miRNA endures across diverse array of plants, animals and fungi by expressing through transcriptional machinery hijack (Schanen and Li, 2011). Evolutionary duplication generates clustered miRNAs which are co-transcribed to primary transcripts and cleaved into multiple miRNAs. Ordinarily, miRNAs are found in three genomic locations such as introns of protein-coding genes, introns of non-coding genes and exons of non-coding genes. As an exception,

others have reported that miRNA genes possess their very own independent transcription units (Liu *et al.*, 2010; Lee, 2013).

Analysis of miRNA genes indicates large numbers of miRNAs decoded within introns of protein coding genes while 30% were reported within exons of long non-protein coding transcripts (Ro *et al.*, 2007). Presence of RNA Polymerase II (Pol II) in miRNA transcription instigated the exploration of miRNA gene structure as promoters and terminators (Cai *et al.*, 2004; Lee *et al.*, 2004).

Many miRNAs regardless intergenic or intronic, possess their very own transcription initiation regions, adding more layers to complexity. Nevertheless, deliberate research has led to the consensus that intragenic miRNAs on the same strand as the host are co-transcribed by Pol II while intergenic miRNAs are transcribed from their own Pol II or RNA Polymerase III (Pol III) promoter (Schanen and Li, 2011).

The Pol III promoters while permitting transcription of miRNAs with the Alu sequences, mammalian wide interspersed repeat (MWIR) or near upstream tRNA sequences interaction, effectuate a wide variety of regulatory options as RNA polymerases regulate differently through different promoters and terminator elements recognition (Brandenstein *et al.*, 2012). The miRNA expression is influenced by transcription factors or methylation in their promoter region insinuating independent regulation mechanisms that lies beyond our view (Winter *et al.*, 2009).

2.6.1 Canonical Pathway of miRNA Biogenesis

MiRNA is synthesised through a pathway known as the canonical pathway as illustrated in Figure 2.3. Within the nucleus, the primary miRNA (pri-miRNA) transcribe contains one or more hairpin structures with a length that exceeds 10 kilobases (Lee *et al.*, 2006).

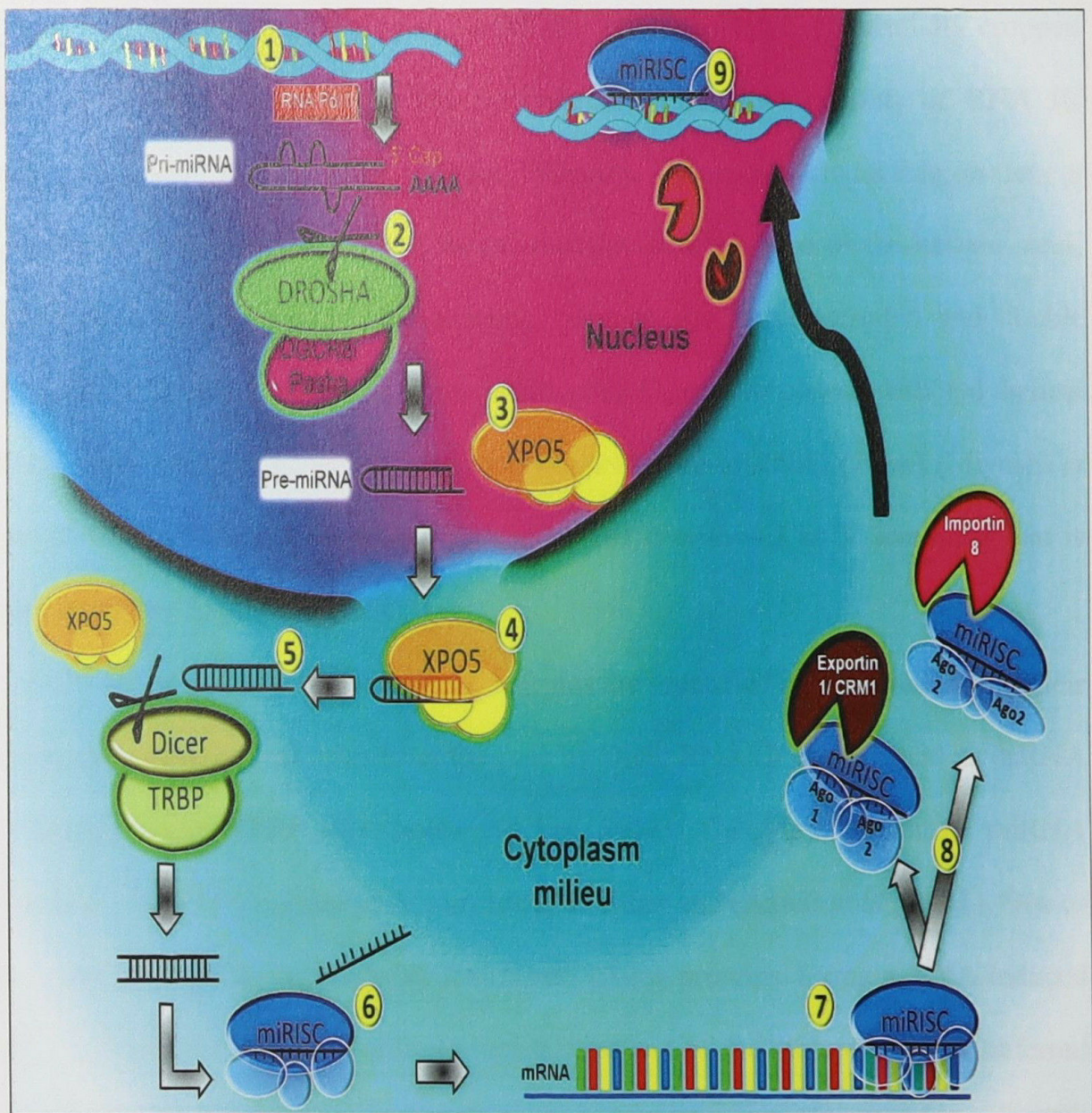


Figure 2.3: Summarising the action of miRNA in nucleus and in cytoplasmic milieu. (1) RNA polymerase II transcribes miRNAs into primary miRNA (pri-miRNA) transcript. (2) Drosha/DGCR8 processes pri-miRNA into precursor miRNA (pre-miRNA). (3) Exportin 5 (XPO5) binds to pre-miRNA to be exported into cytoplasm. (5) Dicer/TRBP processes pre-miRNA into mature miRNA. (6) A complex of Argonaute (Ago) proteins binds to mature miRNA to form miRISC complex, in which one of the miRNA strands is released while the other preferentially get incorporated in the complex. (7) The miRNA guides the complex and post transcriptionally inhibits through 3' UTR binding in messenger RNA (mRNA). (8) In order to proceed with gene regulation, the Ago-miRNA complex will bind to Importin 8 or Exportin 1. (9) The binding of Ago-miRNA complex to chromosomal DNA produces chromatin modifying proteins (CMPs) which lead to increase in H3K4 methylation. This event will activate its respective transcription (Adapted from Vijayarathna *et al.*, 2014).

The pri-miRNA is also 5'-capped, sliced and polyadenylated, sequentially cropped by a multiprotein complex called the microprocessor that consists of RNA III enzyme named Drosha with its cofactor, DiGeorge Syndrome Critical Region Gene 8 (DGCR8)/Pasha. Drosha cleaves the pri-miRNA near the base of the hairpin stem, whereupon Pasha identifies the junction between the single-stranded and double stranded regions at the hairpin base positioning Drosha to cleave with (~1 helical turn). This will then generate a precursor-miRNA (pre-miRNA) (70-nt) (Miyoshi *et al.*, 2010; Rotllan and Fernández-Hernando, 2012) with ~ 2 nt 3' overhang that is recognised by Exportin-5 (XPO5).

In the cytoplasm, pre-miRNA hairpins are identified and cleaved within their stems about two helical turns from the base by Dicer RNA III enzyme and its dsRNA binding partner, TRBP (Westholm and Lai, 2011). This yields a mature miRNA duplex (~21–23 nt) exhibiting 3' overhangs at either end (Axtell *et al.*, 2011). One of the mature miRNA duplex with Argonaute (Ago) proteins forms a RNA-induced silencing complex (RISC) while the opposite strand of the mature miRNA, referred to as miRNA*, is excluded (Miyoshi *et al.*, 2010). The mature miRNA then guides the Ago complex to target transcripts for regulation (Okamura *et al.*, 2007).

Next, the mature miRNA binds to the messenger RNA (mRNA) region through non-specific binding. This substantiates the nature of a single miRNA in governing many mRNA regulations. Specific interaction through binding of 3' UTRs of the target mRNA to the 5' end miRNA's seed region (2-8nt) leads to the translational repression of target mRNAs by either transcript destabilization, translational inhibition, or both (Winter *et al.*, 2009; Rotllan and Fernández-Hernando, 2012).

2.6.2 Non-Canonical Pathway of miRNA Biogenesis

A subset of mature miRNAs was captured through deep sequencing analysis re-entering and predominantly localizing in the nucleus of human cells (Huang and Li, 2012). Other studies have also consistently reported the presence of Ago proteins in the nucleus.

The nuclear-cytoplasmic shuttling of miRNAs employs CRM1/Exportin-1 and Importin-8 together with other carrier proteins (Huang and Li, 2012). Exportin-1 allocates cytoplasmic shuttling of mature miRNA within a complex of Ago 1 and Ago 2 proteins (Liang *et al.*, 2013) while, Importin-8 conversely transports Ago 2 proteins in human cells. The re-entry is performed by miRNA accompanied by its protein effectors (Chen *et al.*, 2012).

In another study, largely translocated miR-29b was found to possess hexanucleotide terminal motif that acts as a transferable nuclear localization element (Hwang *et al.*, 2007; Schanen and Li, 2011). Thereby cytoplasmically routed miRNAs can be imported back into the nucleus for a complete gene regulation. These miRNAs are regarded as highly complementary to promoter sequences (known as promoter-targeting miRNAs), which can connote gene expression in human and mouse cells (Huang and Li, 2012).

The miR-709 imported into mouse nucleus specifically binds to a recognition element on miR-15a/16-1 cluster and blocks the maturation of miR-15a/16-1 at the post-transcriptional level (Tang *et al.*, 2012). Ago-miRNA complex in comparison to RNA inhibition (RNAi) also promotes RNA activation (RNAa). The binding of the Ago-miRNA complex to chromosomal DNA sequences (promoter), conscripts chromatin modifying proteins (CMPs) leading to an increase in H3K4 methylation and thus activates transcription at the targeted promoter (Huang and Li, 2012).

2.7 Cancer, a Life Threatening Disease

Taking into account, 184 countries around the world, the International Agency for Research on Cancer has evinced a report in the year 2012 on the mortality and prevalence cases across major types of cancer within national level. There were 14.1 million new cancer cases, 8.2 million deaths caused by cancer and 32.6 million people living with cancer (within 5 years of diagnosis). It is speculated that, by the year 2030, there will be expected 26 million new cancer cases with 17 million deaths per year (Solowey *et al.*, 2014).

The irrevocable past has it that the ancient civilization of Egypt had a notion of the disease “cancer” as far back as 1600 B.C. and the consensus gentium draws back to Renaissance period upon where cancer was highly apprehended attributing to the first discovery by Sir Rudolf Virchow, a German biologist and politician of cancer cells (Waring, 2015).

The term cancer acuminates a multiform group of diseases traced out by unrestrained cell growth weighty to the emergence of various pathological effects that eventual in death. The occurrence of all forms of cancers coincides with the increase of age factor, yet appearing occasionally in children. In many instances, the abnormal cell growth eventuate in the formation of a macroscopic lump or tumour commonly referred by the Greek as ‘oncos’, thus the term was placed as ‘oncology’ for the study of cancer. This lump commences into larger sizes and kills the patient through a local effect, say occlusion of vital ducts or alimentary tract.

During the post mortem examination, the early physicians denoted the appearance of solid tumours to that of a crab (cancer) due to the irregular and disorganized appearance of the threads of the tumour radiating from the central body. Other forms of cancer nevertheless appear as individual cells diffusing through